

Numerical Simulation of the Two-phase Flow Inside Bubble Columns in the Fully Developed Flow

Pâmela Palhares*, Reginaldo Guirardello

School of Chemical Engineering, University of Campinas, Av. Albert Einstein 500, 13083-852, Campinas-SP, Brazil.
 pamelacoimbrap@gmail.com

This study refers to the simulation and analysis of fluid dynamics in a bubble column in fully developed flow through two numerical approaches, the variational method, and the finite volume method. For simplicity purposes, a zero-order turbulence model was used in the mathematical modelling. Through the proposed methodology, the main components of the circulation inside the column were calculated, e.g., the fluids axial and radial velocities profiles, and the hold-ups profiles. In this work, three cases of two-phase systems were studied, with different column design and operation parameters, which directly impact flow regime inside the column. Two of these cases were carried out with a continuous flow of gas and liquid phases, and one was executed with the liquid phase in semi-batch mode. After evaluations, a similarity between the calculated results was observed, as well as an agreement with literature data, proving the effectiveness of the methodology.

Key words: variational method, finite volume method, fluid dynamics, modelling, hold-up

1. Introduction

Bubble columns are equipment that provide interactions between the gaseous and liquid phases. They are widely used for processes that require slow kinetics reactions (Chaumat et al. 2007), and mass and heat transfer are required due to their high mass and heat transfer coefficients, and other advantages such as low maintenance, operating cost, simple geometry design and absence of moving parts. However, despite of having a simple design, the fluid dynamics within a bubble column is considered complex and strongly dependent of the geometry, flow rates and the potential presence of internal components.

The properties inside the column can be characterized as global and local (Wu and Al-Dahhan, 2001), the latter being the focus of this work, to analyze the radial profiles of the liquid velocity and the gas hold-up, where the hold-up is the volume fraction of each phase distributed along the width of the column, and both velocity and hold-up profiles are related to the heat and mass transfer in the bubble column.

In this work, the prediction of fluid dynamics profiles for bubble columns was performed through numerical methods, using Excel and GAMS softwares, and then the results were compared with data from the literature.

2. Mathematical model

The hydrodynamic in a bubble column are based on the continuity and momentum balance equations, using a Eulerian approach, for a cylindrical column system with axis symmetry. The mass and momentum balance equations for two phase flow can be found in Torvik and Svendsen (1990) and Grienberger and Hofmann (1992). The model applied considers a general pseudo-homogeneous system, with two phases in a fully developed flow and all quantities, e.g., holdups (ε_i), radial velocity (v_{ir}), axial velocity (v_{iz}), varying only in the radial direction. The turbulent viscosity ($\mu^{(t)}$) was calculated using a zero-order turbulence model proposed by Chen et al. (1995) and Menzel et al. (1990). For modelling, it was considered the lift force, also known as magnus force, in the momentum equation to bring more accuracy in the predictions of axial liquid velocity and gas hold-up (Tabib and Roy, 2008), and it was considered equations found in the literature using the liquid density and the radial gradient of the liquid axial velocity, since in practice the liquid is the continuous phase. The mass balance considers the dispersion effect of the phases, which is important to calculate the hold-up profiles.

3. Methodology

The finite volume method (FVM) and the variational method (VM) were the numerical approaches chosen to solve the model to simulate the gas and liquid hold-ups and velocities profiles in the column. The former method is one of the most used methods to calculate fluid dynamics due to its simple and easy derivation, because the equations can be interpreted in physical terms, solving the partial differential equations through an iterative calculation. Meanwhile, the principle of the latter method is to transform a differential equation into an integral equation, mathematically equivalent, by using the Euler-Lagrange equation (Gal-Or et al., 1972).

The variational method applied here is described in Guirardello (2019) and Palhares and Guirardello (2021) and solved with GAMS. In this work, improvements were made in the algorithm of the variational method presented in Palhares and Guirardello (2021), so that now it does not depend on hold-up profile a starting point, obtained by the finite volume method, to run the simulations.

4. Variational formulation

The variational formulation used in this work is based on Guirardello (2019) and Palhares and Guirardello (2021), using the same mathematical model and the same list of symbols. The main difference is the procedure used to calculate the hold-up of the phases, which is described below, where u_i is the axial velocity (v_{iz}) and v_i is the radial velocity (v_{ir}), for phases $i = l, g$. From the continuity equation and the hold-up balance, we have:

$$\frac{1}{\varepsilon_{l1}} \cdot \frac{d\varepsilon_{l1}}{dr} = \frac{v_{l1}}{f(r)} \quad (01)$$

$$\varepsilon_{l1} + \varepsilon_{g1} = 1 \quad (02)$$

where $f(r) = D_{ij}$ (Palhares and Guirardello, 2021), while in the other balance equations it is used $(\varepsilon_{l2}, \varepsilon_{g2})$:

$$\varepsilon_{l2} \cdot v_{l1} + \varepsilon_{g2} \cdot v_{g1} = 0 \quad (03)$$

$$\frac{\dot{m}_i}{\rho_i} = \left[\int_0^R \varepsilon_{i2} \cdot u_{i1} \cdot 2\pi \cdot r \cdot dr \right] \quad i = l, g \quad (04)$$

Also, an auxiliar parameter a is used, with a given value, in the boundary condition:

$$\varepsilon_{l1}(r = R) = a \quad (05)$$

This value is used in the integration of Equation (01) over the interval $(0 \leq r \leq R)$ with the trapezoidal rule:

$$\ln[\varepsilon_{l1}(r_{k-1})] = \ln[\varepsilon_{l1}(r_k)] - \frac{\Delta r}{2} \cdot \left[\frac{v_{l1}(r_{k-1})}{f(r_{k-1})} + \frac{v_{l1}(r_k)}{f(r_k)} \right] \quad (06)$$

The iterative procedure then is given as follows:

0 – Initialization of the iterative procedure.

For $n = 0$, it starts by assigning arbitrary initial values to the quantities $(u_{i2}, v_{i2}, \varepsilon_{i2})^{(n)}$ and the parameter $a^{(n)}$.

1 – Minimization of the functional in the variables $(u_{i1}, v_{i1}, \varepsilon_{i1})^{(n)}$ and parameters $(u_{i2}, v_{i2}, \varepsilon_{i2})^{(n)}$, as described in Guirardello (2019), subject to the restrictions given by (02), (03), (04), (05), and (06), using GAMS/CONOPT.

2 – Stopping criterium (convergence test)

The iterative procedure is repeated, until the following criteria are satisfied (δ is a very small given number):

$$\left| u_{i1}^{(n)} - u_{i2}^{(n)} \right| < \delta \quad i = l, g$$

$$\left| v_{i1}^{(n)} - v_{i2}^{(n)} \right| < \delta \quad i = l, g$$

$$\left| \varepsilon_{i1}^{(n)} - \varepsilon_{i2}^{(n)} \right| < \delta \quad i = l, g$$

which must be satisfied for all integration points ($r_0 = 0, r_1 = \Delta r, \dots, r_M = R$). If not, go to step 3.

3 – Update the values of the quantities $(u_{i2}, v_{i2}, \varepsilon_{i2})^{(n+1)}$ and $a^{(n+1)}$:

$$u_{i2}^{(n+1)} = \omega \cdot u_{i1}^{(n)} + (1 - \omega) \cdot u_{i2}^{(n)} \quad i = l, g \quad (07)$$

$$v_{i2}^{(n+1)} = \omega \cdot v_{i1}^{(n)} + (1 - \omega) \cdot v_{i2}^{(n)} \quad i = l, g \quad (08)$$

$$\varepsilon_{i2}^{(n+1)} = \omega \cdot \varepsilon_{i1}^{(n)} + (1 - \omega) \cdot \varepsilon_{i2}^{(n)} \quad i = l, g \quad (09)$$

where ω is a relaxation factor to guarantee the convergence. Also, update the value of the auxiliar parameter:

$$a^{(n+1)} = a^{(n)} + \gamma \cdot (\lambda_l^{(n)} - \lambda_g^{(n)}) \quad (10)$$

where γ is also a relaxation factor for convergence, and λ_i are the Lagrange multipliers associated to the restrictions given by Equation (4). These Lagrange multipliers are calculated by GAMS.

4 – Update $n \leftarrow n + 1$ and then return to step 1.

It is important to point out that all quantities with index '2' are parameters in GAMS, since these values are kept fixed at each minimization step, while all quantities with index '1' are variables in the minimization with GAMS.

5. Numerical methods

Bubble columns operate with liquid as the continuous phase while gas is the disperse phase and is injected at the bottom of the column. To study its fluid dynamics, two main profiles were analysed, ε_g and v_{lz} , along the radial direction, since there is experimental data in the literature to compare. The other profiles (v_{gz} , v_{lr} , v_{gr}) are calculated, but not compared due to lack of experimental data for them. The simulations were carried out with the systems operating in fully developed flow and without any internal components.

It was evaluated three case studies, varying the column inner diameter and operating conditions. The cases were solved using 40 intervals in the radial direction and using a lift coefficient (C_L) of -1. The values of drag coefficient (C_D) and P'_w/ρ_m were estimated to better fit the calculations to the available experimental data.

The variational method was run in GAMS using the solver CONOPT3 to solve nonlinear equations, while the finite volume method was simulated using the Excel platform to solve the equations with an iterative procedure.

6. Results and discussion

In the previous work (Palhares and Guirardello, 2021), calculations were performed using 20 intervals in the radial direction. However, an analysis was carried out to compare the results obtained with 20, 40 and 80 intervals in the radial direction, for a case study operating in a heterogeneous regime. The analyzed system is the same one presented in case study 2 (Table 2), air and water, based on experimental data from Torvik and Svendsen (1990).

As shown in Table 1, little variation was observed for liquid axial velocity and gas hold-up, and overall, even less variation between 40 and 80 intervals. Therefore, for simplicity's sake, it was chosen to work here with 40 intervals. The values presented in the second and third columns of Table 1 were obtained by the variational method, while in the fourth and fifth columns by the finite volume method.

Table 1 – Mean squared error (all units in CGS).

Number of intervals	Variational Method		Finite Volume Method	
	$\bar{\Delta}\varepsilon_g^2$	$\bar{\Delta}v_{lz}^2$ (cm ² /s ²)	$\bar{\Delta}\varepsilon_g^2$	$\bar{\Delta}v_{lz}^2$ (cm ² /s ²)
20	0.0091	42.5634	0.0099	63.0019
40	0.0026	34.8337	0.0023	56.6509
80	0.0023	32.7273	0.0029	53.4820

Three cases were solved by the proposed methods. The first and second cases considered a system with air and water as gas and liquid phases, with continuous co-current flow, varying only the gas inlet which directly affects the flow regime. The third case operates in a semi-batch mode with the gas phase as a continuous flow.

Table 2 – Cases characteristics.

Case	Fluids	D_c (cm)	U_{s_g} (cm/s)	\dot{m}_g (g/s)	\dot{m}_l (g/s)
1	Air and water	29	4	6.30	658.00
2	Air and water	29	8	3.20	658.00
3	Air and ethanol 0.05%	40	16	24.12	0.00

Table 3 – Fitted parameters.

Case	Variational Method		Finite Volume Method	
	C_D (g/cm ³ .s)	P'_w/ρ_m (cm ² /s ²)	C_D (g/cm ³ .s)	P'_w/ρ_m (cm ² /s ²)
1	32	10450	32	10000
2	40	14700	40	14500
3	20	26600	20	27400

In figures 1, 2 and 3, respectively referring to each case, it is possible to observe the behavior of the axial velocity of the liquid phase (a) and the gas hold-up profile across the column width. Although cases 1 and 2 have the same column design and characterization of fluids, both have different flow regimes, which directly impacts the calculated profiles, since the flow regime is directly linked to the column diameter and the superficial gas velocity (Kantarci et al., 2005).

Because of this difference, it is possible to see a less extensive liquid circulation in Figure 1 (a), and consequently a flatter ε_g curve(b), if compared to that presented in case 2, Figure 2 (b), characteristic of the homogeneous regime, due to the uniformity of bubble dispersion. In the other hand, case 2 although is very close to the transition zone is considered a heterogeneous, and thus present an accentuated v_{Lz} profile. In both cases the calculated results are close to experimental data obtained from literature.

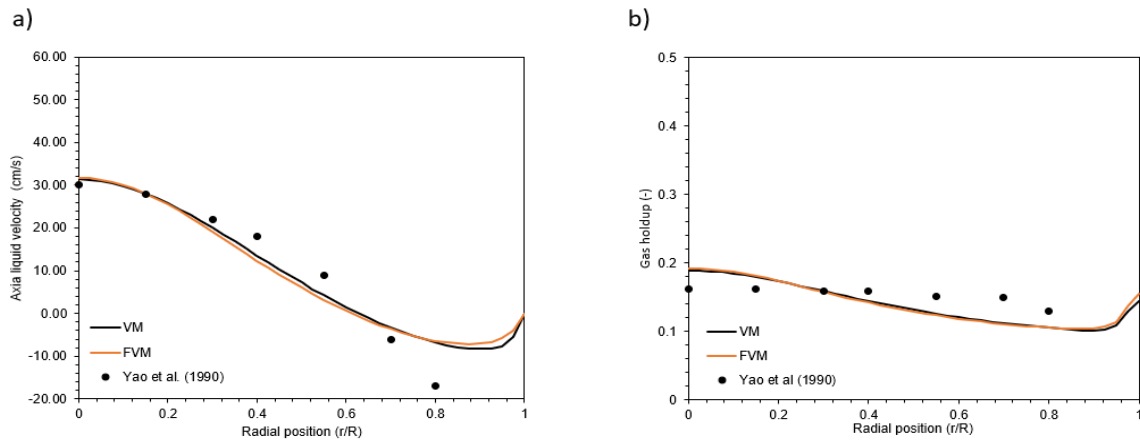


Figure 1 - Results for (a) axial liquid velocity and (b) local gas holdup, comparing with experimental results from Yao et al. (1990).

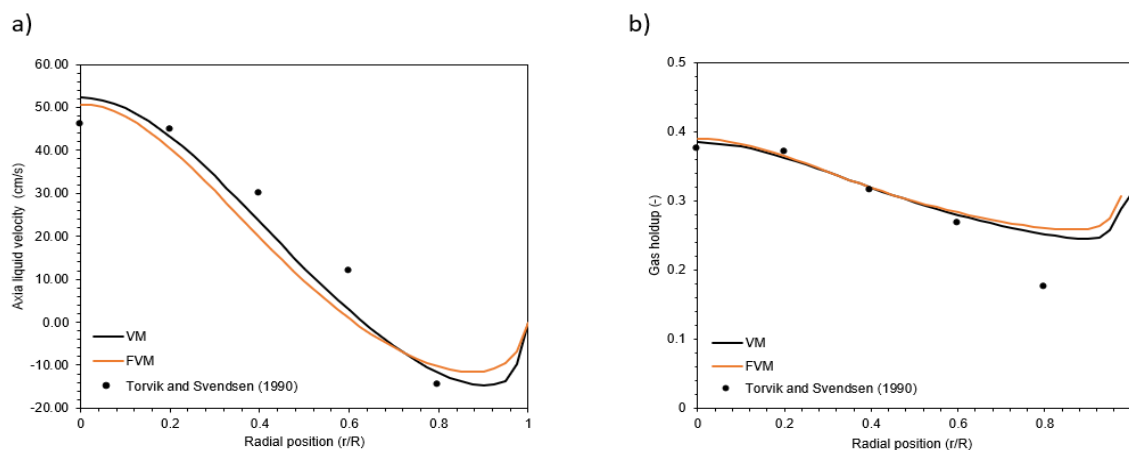


Figure 2 – Results for (a) axial liquid velocity and (b) local gas holdup, comparing with experimental results from Torvik and Svendsen (1990).

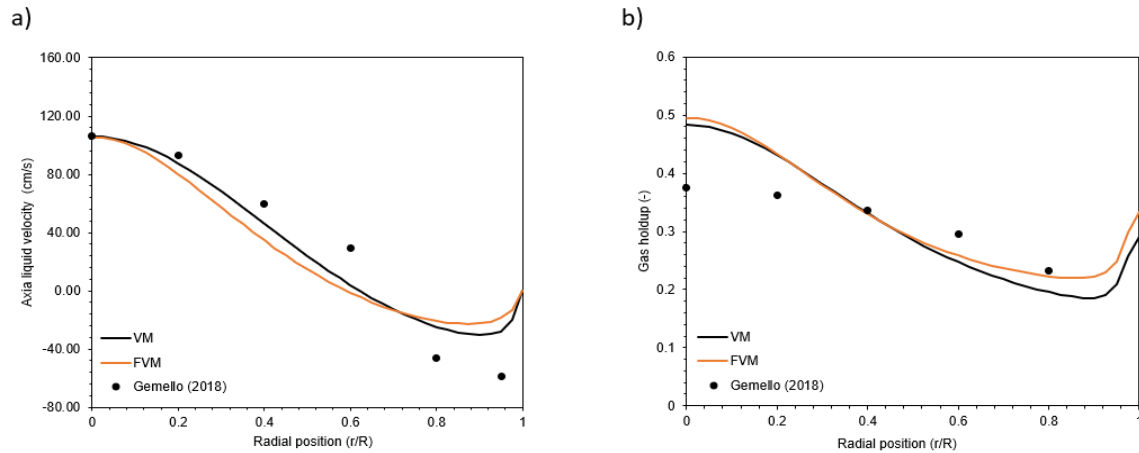


Figura 3 - Results for (a) axial liquid velocity and (b) local gas holdup, comparing with experimental results from Gemello (2018).

In the last case, shown in Figure 3, it is possible to observe the behaviour of system with 0.05% ethanol and air. The simulated column has a column diameter (D_c) of 40cm, operating in semi-batch with a gas inlet velocity of 16cm/s. This system is characterized by the heterogeneous regime, also known as churn-turbulent flow. Although the mathematical model used was mainly developed for a column with continuous flow of both phases, the axial velocity results obtained by both methods were close to the data from literature. Meanwhile, in gas hold-up profile, it was observed that the calculated value in the column center was higher than expected, but it gets closer to Gemello (2018) data in the intermediate points in the radial direction.

Further in the analysis from these results, it was also verified that there is a linear correlation for $C_D \times \max\{\text{abs}[(v_{gz} - v_{lz})]\}$, meaning that the drag coefficient decreases as the difference between the fluids axial velocities increases. This indicates a physical meaning for the fitted parameters, with a quadratic behavior for the drag force. Table 4 presents the difference between v_{iz} for each case and in figure 4 (a) it is possible to notice that C_D varies linearly as Δv_{iz} increases, with an equation for the straight line given by $y = -0.4235x + 49.165$ and a correlation factor of 0.9083.

Table 4 – Maximum difference between v_{iz} .

Case	Δv (cm/s)
1	32.95
2	28.38
3	69.70

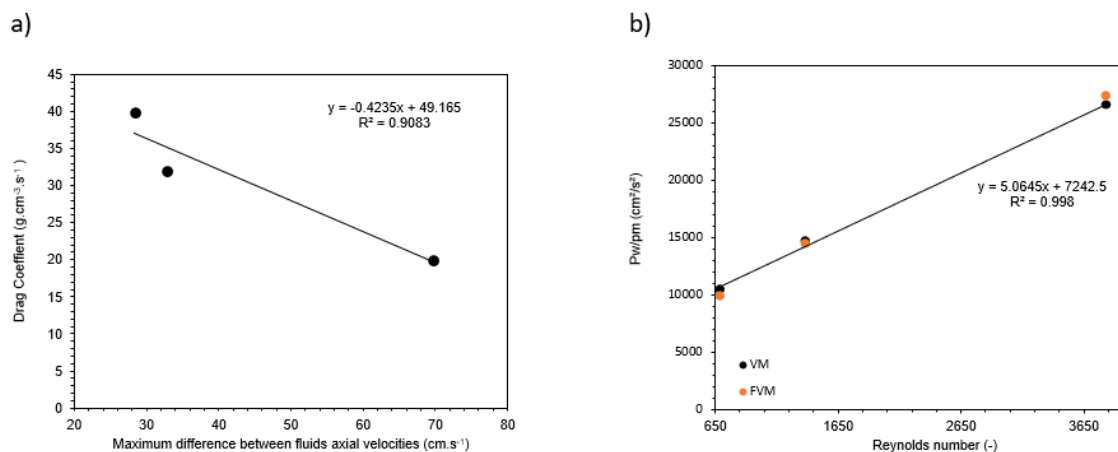


Figure 4 – Correlations between the drag coefficient and the difference gas and liquid velocities (a) and (b) P_w/ρ_m and the Reynolds number.

Although in bubble columns the Reynolds number is often calculated using the bubble diameter, in the present work it was used the classical way to calculate the Reynolds number of the gas phase:

$$Re_g = \frac{\rho_g \cdot D_c \cdot U_{sg}}{\mu_g} = \frac{\rho_g \cdot D_c}{\mu_g} \cdot \frac{\dot{m}_g / \rho_g}{\pi \cdot (D_c/2)^2} \quad (11)$$

Figure 4 (b) shows a strong linearity between the fitted values of P'_w/ρ_m and Re_g , with an almost straight line for the variational method $y = 5.0645x + 7242.5$ and a correlation factor of 0.908, displayed in Figure 4 (b), while for finite volume method the equation for the straight line was $y = 5.465x + 6501.2$ with a correlation factor of 0.998. This indicates a physical behaviour, more than just curve fitting, making the model predictive.

7. Conclusions

The numerical methods used to calculate a two-phase flow in a bubble column showed good results and were compatible with the experimental results obtained from literature. A zero-order turbulence model was assumed to express the liquid dispersion for simplicity purposes, but there are other more elaborated models like the k- ϵ and k- ω models, among others. Nonetheless, the model used was able to represent the experimental data. In this study, all physical properties were considered constant, but in future research the calculations could be revised in case of chemical reaction or if physical properties change with pressure.

The results presented here for the variational method are more accurate than those presented in previous works (Guirardello, 2019; Palhares and Guirardello, 2021), due to improvements in the calculation of the hold-up, resulting in an algorithm with much better convergence, no longer having dependency on previous results from the finite volume method, used as initial parameters to run GAMS in the previous works. One important feature is Equation (10), which guarantees that $\lambda_l = \lambda_g$, since both should be equal to $-dp/dz$ at the stationary condition, so that the resulting equations are equal to the momentum equations for both phases.

Finally, it was verified a correlation between the fitted model parameters and some properties of the system, such as Reynolds number for P'_w/ρ_m and relative velocities for C_D . This makes the model predictive, so that for other operating conditions the values of these parameters can be estimated. However, the case studies were all for air-water systems, and so for other gas-liquid systems these parameters may behave differently.

Acknowledgments

The authors gratefully acknowledge the financial support of CNPq – Brazil, process number 142731/2019-6.

References

- Chaumat, H., Billet, A. & Delmas, H., 2007, Hydrodynamics and mass transfer in bubble column: Influence of liquid phase surface tension, *Chemical Engineering Science* 62, 7378–7390.
- Chen Z., Zheng C., Feng. Y., 1995, Modelling of three-phase fluidized beds based on local bubble characteristics measurements, *Chemical Engineering Science*, 50, 231–236.
- Gal-Or B, Wheihls D., 1972, Variational analysis of high mass transfer rates from spherical particles boundary layers, *Int. J. Mass Heat Transfer*, 15,2027-2044.
- Gemello L., 2018, Modelling of the hydrodynamics of bubble columns using a two-fluid model coupled with a population balance approach, PhD Thesis, Université de Lyon, France.
- Grienberger J., Hofmann H., 1992, Investigations and modelling of bubble columns, *Chemical Engineering Science*, 47, 2215–2220.
- Guirardello R., 2019, A Numerical Resolution of Fluid Dynamic Problems Using a Saddle Point Variation Formulation, *Chemical Engineering Transactions*, 74, 1015-1020.
- Kantarci N., Boral F., Ulgen K.O., 2005, Bubble column reactor, *Process Biochemistry*, 40, 2263-2283.
- Menzel T., Weide T., Staudacher O., Wein O., Onken U., 1990, Reynolds's shear stress for modeling of bubble column reactors, *Ind. Eng. Chem. Res.*, 29, 988–994
- Palhares P., Guirardello R., 2021, Numerical Simulation of Hold-Up and Velocity Profiles for Two-Phase Developed Flows in a Column, *Chemical Engineering Transactions*, 86, 1189- 1194.
- Tabib M.V., Roy S.A., Joshi J.B., 2008, CFD simulation of bubble column—an analysis of interphase forces and turbulence models, *Chemical Engineering Journal*, 139, 589-614.
- Torvik R., Svendsen H.F., 1990, Modelling of slurry reactors. A fundamental approach, *Chemical Engineering Science*, 45, 2325–2332.
- Yao B.P., Zheng C., Gasche H. E., Hofmann H., 1991, Bubble behaviour and flow structure of bubble columns, *Chemical Engineer Process*, 29, 65-75.
- Wu Y., Al-Dahhan M.H., 2001 Prediction of axial liquid velocity profile in bubble column, *Chemical engineering Science*, 56, 1127-1130.